05.3;06.5

Thermal conductivity of a composite based on *n*-alkane and nanosized additives

© V.M. Egorov, A.K. Borisov, V.A. Marikhin

Ioffe Institute, St. Petersburg, Russia
E-mail: victor_egorov1@inbox.ru

Received June 10, 2021
Revised September 16, 2021
Accepted September 27, 2021

Composites based on *n*-alkane and nanoscale additives were investigated to determine the efficiency of heat transfer during phase transitions in phase change materials. There was justified a new technique for obtaining thermal conductivity by analyzing shapes of the peaks recorded in thermograms by the method of differential scanning calorimetry. It was found that the thermal conductivity of composite materials is several times higher than the thermal conductivity of the initial *n*-alkane. The observed effect is due to the specificity of the supramolecular nanostructure of the composite, which differs from the supramolecular structure of the nonadecane.

Keywords: conductivity, composite, phase transitions, n-alkane.

DOI: 10.21883/TPL.2022.01.52469.18915

One of the most topical and promising directions of the green energetics evolvement is developing PCMs (phase change materials) able to absorb, store and transform the heat energy fluxes due to their own thermal effects, including those occurring during phase transitions (PT). As PCMs most promising in this regard, homologous series of aliphatic hydrocarbons and their derivatives are considered, normal n-alkanesfirst of all [1–3]. Besides the most important PCM characteristics, namely, their energy absorption capacity, very important is their thermal conductivity defining the capacity of energy absorption or emission in the form of heat. Widespread acceptance of the method of differential scanning calorimetry (DSC) caused by its rapidity and informativeness allowed development of a method for determining thermal conductivity coefficients of various materials: polymers, metals, ceramics [4]. This method is based on analyzing shapes of the peaks of heat capacity $C_p(T)$ induced by phase transitions (solid−solid transitions, melting) and on comparing those peaks with heat capacity peaks in reference materials.

In this work, the following composites based on *n*-alkane (nonadecane) and nanoscale additives were used to reveal the efficiency of heat conversion during phase transitions: initial nonadecane (sample I), nonadecane with added particles of Al_2O_3 50−70 nm in size (sample II), nonadecane with added particles of Al_2O_3 90−110 nm in size (sample III), nonadecane with added particles of Ag 90−100 nm in size (sample IV). The composite samples were prepared at the nonadecane/powder weight ratio of 95/5. To uniformly distribute the additives over the volume, melted samples were processed with ultrasonic dispergator UZD1−0,1/22.

Thermodynamic parameters of the composite were determined with calorimeter DSC-500 („Spetspribor“) in the nitrogen atmosphere at the scanning speed of 1 K/min. The temperature scale was calibrated with respect to the melting points of ice (273.1 K) and indium (429.7 K), the heat flux scale was calibrated with respect to the leucosapphire heat capacity. The measurements were performed in the temperature range of 270−440 K. Weight of the test samples was 5 mg.

As noticed above, in work [4] a method was developed for determining the thermal conductivity coefficient by analyzing the shape of the phase transition endothermic peak. It was shown that inclination of the peak in the experimental DSC curve of the test sample and the shift of the peak position $T_{\max}$ towards higher temperatures (the so called thermal delay) were governed by thermal resistance R. Parameter R is composed of the calorimeter cell thermal resistance R_0 and test sample thermal resistance R_s ($R = R_0 + R_s$) and is defined by relation $R = \operatorname{ctg}\varphi$ where φ is the front edge inclination angle of the heat capacity peak in the DSC curve.

The calorimeter cell thermal resistance R_0 depends on its design features and will be determined experimentally for each calorimeter using calibration with respect to references. Fig. 1 (curve *5*) represents the melting endotherm of the reference indium sample placed directly inside the capsule (as the reference, the Wood's alloy and gallium may be also used). The figure shows that the endotherm front edge remains linear when the temperature increases and, hence, thermal resistance remains constant in the process of melting. This allowed determining R_0 that appeared to be $91\,\mathrm{K}\cdot\mathrm{W}^{-1}$ for the given calorimeter. Thus, using test samples of materials possessing well pronounced anomalies of the heat capacity dependence on temperature (e.g., in the form of a solid−solid transition), it is possible to derive the sample thermal resistance R_s from difference $R - R_0$. Therewith it is necessary to retain the same test conditions as in testing the reference sample, namely, heating rate,

Thermal conductivity coefficient in nonadecane with additives and calculation parameters of heat capacity peaks arising during a solid−solid transition

Sample	R, $K \cdot W^{-1}$	R_s, $K \cdot W^{-1}$	λ, $W \cdot m^{-1} \cdot K^{-1}$	T_{01}, T_{02}, K	ΔC_{max}, $J \cdot g^{-1} \cdot K^{-1}$	q_1, q_2, $J \cdot g^{-1}$	$q_n/(q_1+q_2)$, %	B	ω, nm^3
I	979	888	0.1264 [5]	291.60	18.0	35.1	77	580	84
				292.40	11.0	10.8	23	1200	570
II	299	208	0.5376	292.50	15.0	17.5	44	1000	290
				293.15	43.0	21.9	56	2300	540
III	317	226	0.4928	292.50	16.0	18.7	40	1000	280
				293.1	43.0	27.6	60	2200	500
IV	364	273	0.4032	291.75	10.0	11.7	38	1000	430
				292.30	38.0	19.3	62	2300	600

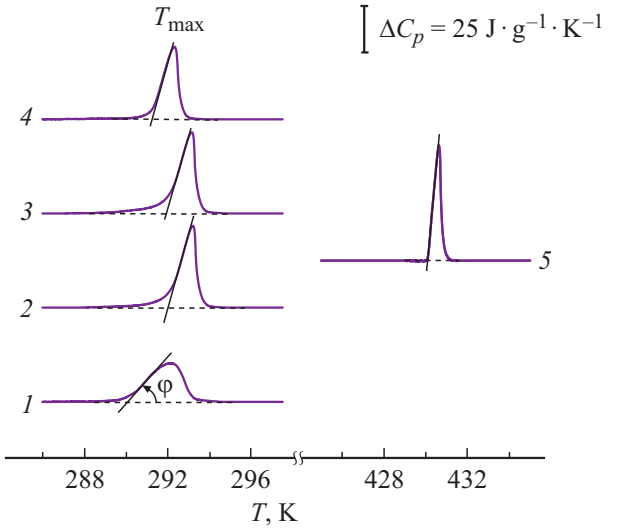

Figure 1. Endothermic peaks allowing for solid−solid transitions in samples I−IV (curves *1*−*4*, respectively), and in the reference In sample (curve *5*). Bold lines represent experimental data, fine lines are linear extrapolations of the peak front edge, dashed lines correspond to the zero ordinate.

standard capsules, and gas purging mode for the DSC calorimetric chamber.

The R_s value determines the sample material thermal conductivity coefficient λ according to relation $\lambda = d/R_s$ accurately to factor d allowing for the sample geometric dimensions. In testing samples of the same geometric shape, factor d remains constant. This allows revealing comparative characteristics of the thermal conductivity of the test samples. If the thermal conductivity coefficient is known for one of the samples, it is possible to find d from R_s established for this sample and then use this d in calculating λ for other samples.

Fig. 1 presents DSC curves obtained in heating the test samples in the temperature interval embracing the range of the first−kind structural PT ($\sim 290-294$ K). The figure shows that the shapes of the endothermic peaks in the curves corresponding to nonadecane (curve *1*) and composites (curves *2*−*4*) are quite different: the last ones exhibit a great increase in the peak amplitudes ($\Delta C_{p\,max}$) and shrinkage of the phase transformation temperature ranges. The figure also shows that, when the temperature increases, the endotherm front edges remain linear to a high extent for all the samples and, hence, thermal resistance remains constant in the process of the phase transition. The R values presented in the table were derived for all the test samples from the front edge inclination angle φ.

As noticed above, to determine coefficients λ for all the samples it is sufficient to find d for only one of the test samples. Indeed, since the paraffin thermal conductivity coefficient is well known ($\lambda = 0.1264\ W \cdot m^{-1} \cdot K^{-1}$ [5]), it is easy to find the factor allowing for the sample geometric dimensions; for nonadecane, this factor appeared to be $d = 112\ m^{-1}$. Knowing this value, it is possible to find the thermal conductivity coefficient for the composites under study. The λ values calculated in this way are listed in the table.

Data listed in the table bring us to the conclusion that thermal conductivity (thermal conductivity coefficient λ) of the studied composites essentially (3−4 times) exceeds the thermal conductivity of most amorphous/crystalline polymers. Notice that data obtained for two composites with the same amounts of added Al_2O_3 particles 50−70 and 90−110 nm in size differ significantly from each other. In the first case, the thermal conductivity appeared to be somewhat higher than in the second case.

The most prominent effect of introducing nanoscale particles was observed in the study when $\sim 10\%$ of graphene was added to paraffin [6]. As per that study, the thermal conductivity coefficient was $\lambda = 0.9362\ W \cdot m^{-1} \cdot K^{-1}$. Since the solid body thermal conductivity is of different natures depending on the substance type, it is possible to assume that adding to paraffin particles of silver and aluminum oxide possessing considerably higher conductivity ($_2O_3$ $\lambda \approx 25-30\ W \cdot m^{-1} \cdot K^{-1}$ for Al, $\lambda \sim 400\ W \cdot m^{-1} \cdot K^{-1}$ for Ag) may lead to an increase in the composite thermal conductivity. As being of additive character, thermal resistance is a sum of thermal resistances of paraffin and additive. Assuming the latter to be almost zero, we may expect insignificant decrease in the composite thermal resistance and, hence, an increase in thermal conductivity.

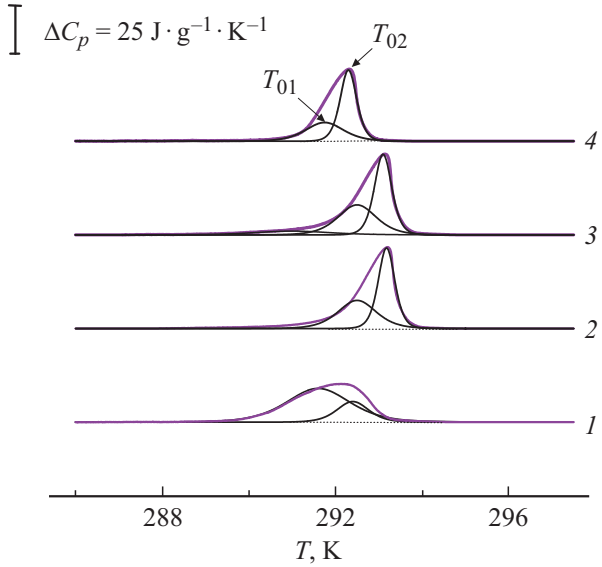

Figure 2. Endothermic peaks allowing for the first−kind solid−solid transitions in samples I−IV (curves *1*−*4*, respectively). Bold lines represent experimental data, fine lines represent the calculations obtained through relation (2).

Our estimates have shown that the effect of this increase cannot exceed 5−10%. Therefore, the observed effect of the multiple increase in the composite thermal conductivity coefficient is obviously connected with modification of the paraffin structure due to introducing small particles into it. This fact manifests itself in variations in thermodynamic parameters of the solid−solid transition.

Fig. 1 demonstrates the asymmetry of the peak shapes which may be caused by the existence of at least two components. To reveal those components, the peaks were analyzed in the framework of the thermodynamic self-consistent field theory [7] in respect to the Λ-like smeared first−kind PT. The main idea is that in the bulk of the old phase there occurs localization of multiple fluctuations within a limited space in the form of stable nuclei of the new phase, namely, the so called elementary volumes of phase transformation ω. In further progress of the transition, the phase interface displacement is ensured by subsequently adding nuclei with volume ω to the emersed phase interface. Size of stable nuclei ω may be derived from the shapes of $C_p(T)$ peaks. In work [8], the relation describing the temperature dependence of thermal conductivity for a smeared phase transition was obtained in the following form:

$$\Delta C_p(T) = 4\Delta C_{\max} \exp[B(T - T_0)/T_0] \times \left[1 + \exp[B(T - T_0)/T_0]\right]^{-2}, \quad (1)$$

where T_0 is the temperature of the first−kind PT, $\Delta C_{\max}$ is the maximum heat capacity at $T = T_0$, B is the athermal parameter.

Asymmetric peaks were decomposed [3] into two symmetric Λ-like peaks under the assumption that the enthalpy of the experimentally obtained peak (q_n) is a sum of enthalpies of two symmetric peaks ($q_1 + q_2$), namely, $q_n = q_1 + q_2$. By varying parameters T_0, $\Delta C_{\max}$ and B, it was possible to gain coincidence of each symmetric peak with either the right peak shoulder (high−temperature shoulder with $T_0 = T_{02}$) or with the left one (low−temperature shoulder with $T_0 = T_{01}$). The best agreement between the calculated and experimental dependences was observed at the parameter values listed in the table. Fig. 2 presents the Λ-like peaks calculated via relation (2) and experimental temperature dependences of heat capacity $\Delta C_p(T)$. Parameter B of the above-presented relation (1) bears the most interesting information on the PT physical nature since it is connected with the value of the heat capacity peak $\Delta C_{\max}$

$$\Delta C_{\max} = q_0 B/4T_0 \quad (2)$$

(where q_0 is the transformation temperature) and with the transformation elementary volume ω

$$B = \omega\rho q_0/kT_0 \quad (3)$$

(where k is the Boltzmann constant, ρ is the density).

Parameter B appeares to be a structure−sensitive parameter since it defines the volumes of the new phase nuclei in the materials with smeared PTs. Using relation (2), it is possible to obtain the transformation specific heat (enthalpy), relation (3) gives the transformation elementary volume ω (assuming in the first approximation that the paraffin crystal density is $\rho \sim 0.8\,\mathrm{g \cdot cm^{-3}}$ [9]). The calculations obtained via those relations are presented in the table.

Indeed, the nonadecane solid−solid transition proceeds in to stages. As Fig. 2 shows, phase transformation in the major part of the initial nonadecane crystal takes place at the first stage. At the same time, origination of the new phase domains $\omega = 84\,\mathrm{nm}^3$ in size is initiated (this follows from the ratio between the transformation heat values at the first and second stages; see the table). The phase transformation leads to depletion of defect−free crystal regions and increase in the surface energy because of accumulation or emergence of obstacles in the remaining, i. e., not subjected to the transformation, part of the crystal. At the second stage of the phase transition, the phase transformation of the initial nonadecane proceeds in the lesser (remaining) part of the crystal with the increase in the nuclei volume to $\omega = 570\,\mathrm{nm}^3$.

The table shows that, in contrast with the case of initial nonadecane, phase transformation in composites takes place mainly in the larger part of the crystal in defect−free regions with large volumes ($\omega = 500$−$600\,\mathrm{nm}^3$), which leads to reduction of the phonon scattering [5] and promotes an increase in the composite crystal thermal conductivity relative to that in the initial nonadecane. In the defect−free regions with large volumes, a lamellar structure arises, which is better ordered as compared with the initial matrix

due to the increase in the lamella width. The latter needs experimental validation.

Therefore, it has been established that the significant increase in thermal conductivity is caused not by the „additive“ introduction of a more heat−conductive material but by reconstruction of the nonadecane supramolecular structure due to the presence of additional crystallization centers and formation of a specific supramolecular structure of *n*-alkane in the composite.

Conflict of interests

The authors declare that they have no conflict of interests.

References

[1] V.M. Egorov, A.K. Borisov, V.A. Marikhin, Tech. Phys. Lett., **45** (12), 1204 (2019). DOI: 10.1134/S1063785019120058.
[2] A.K. Borisov, V.M. Egorov, V.A. Marikhin, J. Phys.: Conf. Ser., **1236**, 012010 (2019). DOI: 10.1088/1742-6596/1236/1/012010
[3] V.M. Egorov, A.K. Borisov, V.A. Marikhin, Phys. Solid State, **63** (3), 498 (2021). DOI: 10.1134/S1063783421030069.
[4] V.A. Bershtein, V.M. Egorov, *Differential scanning calorimetry of polymers: physics, chemistry, analysis, technology* (Ellis Horwood, N.Y., 1994).
[5] Yu.K. Godovsky, *Teplofizika polimerov* (Khimiya, M., 1982) (in Russian).
[6] M. Li, Appl. Energy, **106**, 25 (2013). DOI: 10.1016/j.apenergy.2013.01.031
[7] M. Fisher, *Priroda kriticheskogo sostoyaniya* (Mir, M., 1968) (in Russian).
[8] G.A. Malygin, Phys. Solid State, **43** (10), 1989 (2001). DOI: 10.1134/1.1410644].
[9] D.M. Small, *Physical chemistry of lipids* (Plenum Press, N.Y.−London, 1986).